



Clobenpropit analogs as dual activity ligands for the histamine H₃ and H₄ receptors: Synthesis, pharmacological evaluation, and cross-target QSAR studies

Herman D. Lim^{a,†}, Enade P. Istyastono^{a,†,‡}, Andrea van de Stolpe^a, Giuseppe Romeo^a, Silvia Gobbi^a, Marjo Schepers^a, Roger Lahaye^a, Wiro M. B. P. Menge^a, Obbe P. Zuiderveld^a, Aldo Jongejan^a, Rogier A. Smits^a, Remko A. Bakker^a, Eric E. J. Haaksma^{a,b}, Rob Leurs^a, Iwan J. P. de Esch^{a,*}

^aLeiden/Amsterdam Center for Drug Research (LACDR), Division of Medicinal Chemistry, Department of Pharmacochimistry, Faculty of Exact Sciences, VU University Amsterdam, De Boelelaan 1083, 1081 HV Amsterdam, The Netherlands

^bBoehringer Ingelheim RCV GmbH & Co. KG, Dr. Boehringergasse 5-11, Vienna, Austria

ARTICLE INFO

Article history:

Received 16 January 2009

Revised 1 April 2009

Accepted 6 April 2009

Available online 11 April 2009

Keywords:

Histamine H₃ receptor

Histamine H₄ receptor

GPCR

Cross-target QSAR

Selectivity

Clobenpropit analogs

ABSTRACT

Previous studies have demonstrated that clobenpropit (*N*-(4-chlorobenzyl)-*S*-[3-(4(5)-imidazolyl)propyl]isothiourea) binds to both the human histamine H₃ receptor (H₃R) and H₄ receptor (H₄R). In this paper, we describe the synthesis and pharmacological characterization of a series of clobenpropit analogs, which vary in the functional group adjacent to the isothiourea moiety in order to study structural requirements for H₃R and H₄R ligands. The compounds show moderate to high affinity for both the human H₃R and H₄R. Furthermore, the changes in the functional group attached to the isothiourea moiety modulate the intrinsic activity of the ligands at the H₄R, ranging from neutral antagonism to full agonism. QSAR models have been generated in order to explain the H₃R and H₄R affinities.

© 2009 Published by Elsevier Ltd.

1. Introduction

There are four known histamine receptor subtypes, which all belong to the class of G-protein-coupled receptors (GPCRs). Antagonists for the histamine H₁ receptor (e.g., fexofenadine and ι -cetirizine) and the histamine H₂ receptor (e.g., cimetidine and ranitidine) have been used very successfully in the clinic for the treatment of allergic conditions and gastric ulcer, respectively. The potential clinical applications for ligands of the histamine H₃ receptor (H₃R) and the histamine H₄ receptor (H₄R) are being studied intensively. The H₃R was first described in 1983 as a presenaptic autoreceptor that was predominantly (but not exclusively) expressed in the brain.¹ Stimulation of this receptor inhibits the synthesis and the release of histamine from histaminergic neurons. The H₃R also modulates other neurotransmitter systems, for example, dopaminergic, serotonergic, and cholinergic systems, both in the central and peripheral nervous systems. The development of H₃R targeting drugs received a major boost when the gene that en-

codes the receptor was cloned in 1999. Currently, several H₃R ligands are in clinical studies for a wide variety of applications, including Alzheimer's disease, obesity, and epilepsy.²

Following the cloning of the H₃R gene, several groups identified and characterized the H₄R that was found in the human genome databases based on its homology to the H₃R sequence (37% in the entire sequence and 68% within the transmembrane domains).³ The H₄R is expressed mainly in the peripheral tissues and cells of the immune system.⁴ The H₄R receptor is involved in chemotaxis of eosinophils and mast cells toward the sites of inflammation. Currently, the application of H₄R ligands in the treatment of asthma, allergic rhinitis (hay fever), and pruritis (itch) is being intensively investigated in preclinical studies.⁵

In recent years, considerable progress has been made in the development of ligands selective for the H₃R and the H₄R. The endogenous ligand histamine has high affinity for both receptors. Also several structural analogs of histamine have dual H₃R and H₄R activity, for example, the H₃R and H₄R agonist imetit, the H₃R antagonist and H₄R agonist clobenpropit, and the H₃R and H₄R inverse agonist thioperamide have been important as early reference compounds for H₃R and H₄R research (Fig. 1).

To enable a focused study, using cross-target QSAR analysis, we synthesized a series of new clobenpropit derivatives that were tested for their H₃R and H₄R affinity and activity. Subtle differences

* Corresponding author. Tel.: +31 20 5987600; fax: +31 20 5987610.

E-mail address: ideesch@few.vu.nl (I.J.P. de Esch).

† These authors contributed equally to this work.

‡ Original affiliation: Faculty of Pharmacy, Sanata Dharma University, Paingan, Yogyakarta 55281, Indonesia.

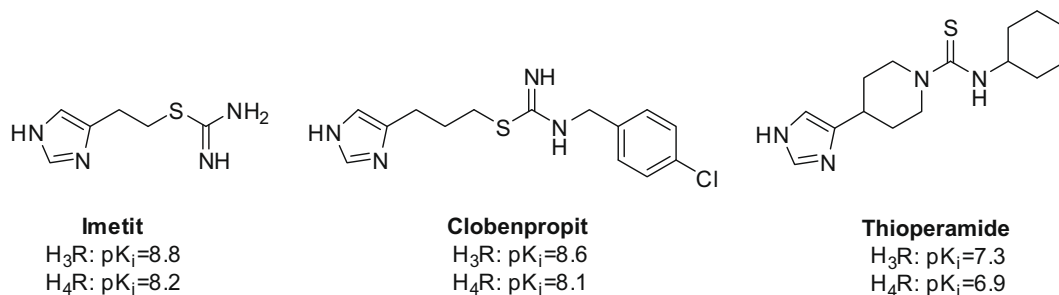


Figure 1. The first generation of H₃R and H₄R reference compounds. Affinity values were taken from Lim et al.²⁰

in structure–activity relationships (SAR) are described. Our efforts to quantify the physical–chemical properties that influence H₃R and H₄R affinity are a first step to more accurately describe the differences in the clobenpropit-binding site of these two receptors.

2. Chemistry

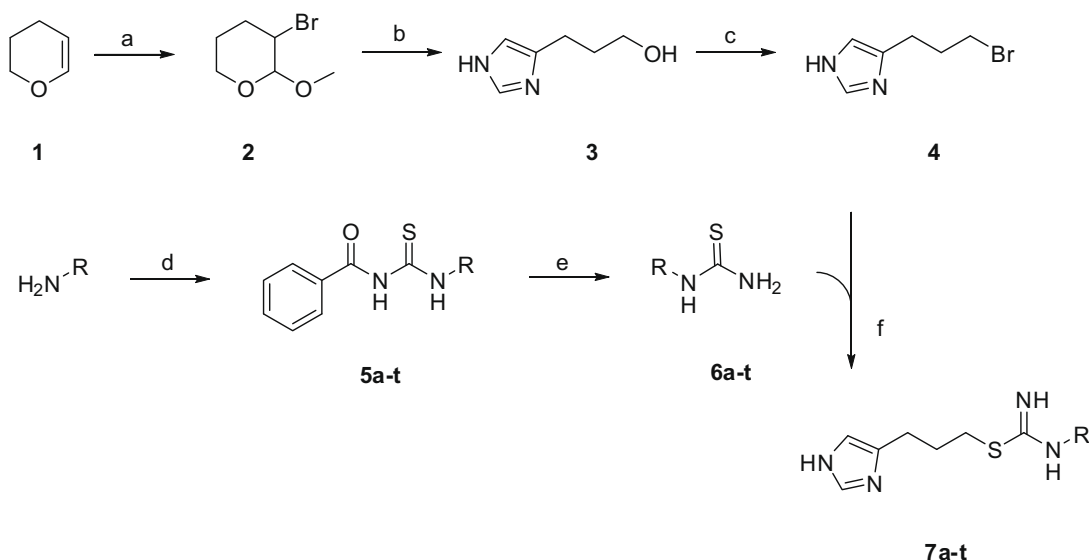
The clobenpropit analogs were synthesized according to a modified literature procedure (Scheme 1).^{6,7} First, 3,4-dihydropyran was treated with sodium acetate, methanol, and bromine to obtain adduct **2** in good yield (58%). This compound was converted to the imidazole-containing intermediate **3** by treatment with formamidine acetate and formamide under reflux conditions. Heating this material with hydrobromic acid resulted in 90% yield of key intermediate **4**.

Diversity was introduced via the use of different amines that were reacted with benzoyl isothiocyanate. The resulting N-benzoyl-N'-R-thiourea compounds **5** were deprotected under basic conditions, leading to thioureas **6** in yields of 47–95%. Combining key intermediate **4** with a range of thioureas **6** gave the final clobenpropit analogs **7**. Conversion of the last step was complete, but isolated chemical yields were only moderate (15–40%) due to the purification by crystallization of the corresponding salts. Isothiourea analogs **7a** and **7d**, as well as guanidine analogs **8a** and **8b** (see Table 1) were synthesized as previously described in literature.^{6,7}

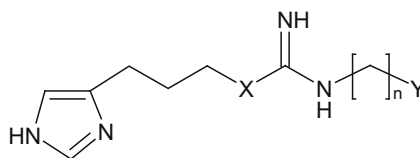
3. Structure–affinity relationship (SAR)

The investigation of the clobenpropit analogs focused on mono-substitution of the isothiourea moiety with variation in the spacer between the isothiourea group and the phenyl moiety and variation in the substituent of the phenyl moiety as shown in Table 1. This structural variation is restricted by taking into account only clobenpropit derivatives that have a spacer length of three methylene (–CH₂–) units between the basic groups of the compounds, that is, the imidazole ring and the isothiourea or guanidine moiety. It is believed that these particular derivatives can obtain a binding mode that allows an interaction similar to that of the endogenous ligand, that is, the basic groups of the ligand interact with Asp3.32 and Glu5.46 (present in both H₃R and H₄R), as we have previously described in ligand-based and structure-based models.^{8–10} Although these interactions can explain the affinity, the intrinsic activities of the ligands results from very subtle differences in structure of the compounds and conformation of the receptor and are more difficult to model.⁹

In general, most of the compounds have good affinity for both the H₃R and the H₄R, with most compounds being more selective for the H₃R. The replacement of the isothiourea group by a guanidine moiety (compare **7b** and **8a**) is unfavorable for the H₃R affinity and results in a compound that shows preference for H₄R. Elongating the spacer between the isothiourea group and the phenyl moiety (compare **7b**, **7l**, **7s**, and **7t**) decreases the affinity, for both the H₃R and H₄R. The substituent of the benzyl substituted compounds



Scheme 1. Reagents and conditions: (a) CH₃COONa, MeOH, Br₂, –50 °C; (b) CH₄N₂·C₂H₄O₂, HCONH₂; reflux; (c) 48% HBr, reflux; (d) benzoyl isothiocyanate, Et₂O, 0 °C; (e) K₂CO₃, EtOH, reflux; (f) EtOH, reflux.

Table 1The affinity of clobenpropit analogs (pK_i) at the human H_3R and the human H_4R , and the intrinsic activity (α) at human H_4R^a 

Compound	<i>n</i>	X	Y	pK_i H_3R	pK_i H_4R	ΔpK_i^b	α H_4R
7a	0	S	H	8.6 ± 0.1	7.9 ± 0.1	0.7	0.59
7b	1	S	Phenyl	8.1 ± 0.1	7.6 ± 0.1	0.5	0
8a	1	NH	Phenyl	7.1 ± 0.1	7.6 ± 0.1	−0.5	0.56
7c	1	S	4-F-phenyl	8.3 ± 0.1	7.6 ± 0.1	0.7	0.39
7d^c	1	S	4-Cl-phenyl	8.5 ± 0.1	8.0 ± 0.1	0.5	0.83
7e	1	S	3-Cl-phenyl	8.1 ± 0.1	7.8 ± 0.1	0.3	0.48
7f	1	S	2-Cl-phenyl	8.1 ± 0.1	8.0 ± 0.1	0.1	0.15
7g	1	S	3,4-Dichloro-phenyl	8.2 ± 0.1	8.8 ± 0.1	−0.6	1.00
7h	1	S	4-Br-phenyl	8.6 ± 0.1	8.0 ± 0.1	0.6	0.91
7i	1	S	4-I-phenyl	8.5 ± 0.1	8.0 ± 0.1	0.5	0.98
7j	1	S	4-CH ₃ -phenyl	8.2 ± 0.1	7.6 ± 0.1	0.6	0.46
7k	1	S	4-OCH ₃ -phenyl	8.1 ± 0.1	7.9 ± 0.1	0.2	0.91
7l	2	S	Phenyl	7.7 ± 0.1	7.2 ± 0.1	0.5	0.46
7m	2	S	4-Cl-phenyl	8.0 ± 0.1	7.5 ± 0.1	0.5	0.35
7n	2	S	4-Br-phenyl	8.1 ± 0.1	7.4 ± 0.1	0.7	0.26
7o^d	2	S	4-I-phenyl	8.1 ± 0.1	7.8 ± 0.1	0.3	0.18
7p	2	S	4-CH ₃ -phenyl	7.9 ± 0.1	7.0 ± 0.1	0.9	0.28
7q	2	S	4-OCH ₃ -phenyl	7.7 ± 0.1	6.8 ± 0.1	0.9	0.26
8b	1	NH	2,2-Diphenylvinyl	6.5 ± 0.1	6.8 ± 0.1	−0.3	n.d.
7r	2	S	Diphenylmethyl	7.5 ± 0.1	7.6 ± 0.1	−0.1	0.70
7s	3	S	Phenyl	8.0 ± 0.1	7.3 ± 0.1	0.7	0.44
7t	4	S	Phenyl	7.7 ± 0.1	7.2 ± 0.1	0.5	0.36

n.d., not determined.

Data shown are mean ± SEM of at least 3 independent experiments.

^a SK-N-MC cells stably expressing H_3R or H_4R were used to determine ligand affinities for either the H_3R or the H_4R and the intrinsic H_4R activity.^b $\Delta pK_i = pK_i$ $H_3R - pK_i$ H_4R .^c Clobenpropit.^d Iodophenpropit.

(**7b–k**, **8a**) and the phenethyl substituted compounds (**7l–t**, **8b**) give similar pattern of the affinity changes. However, most of the phenethyl substituted compounds display lower affinity for both the H_3R and the H_4R than in the benzyl substituted compounds.

Introduction of a halogen atom at the 4-position of the benzyl moiety increases the affinity for both the H_3R and the H_4R . Thus, the selectivity remains similar. Interestingly, the increase in affinity at the human H_4R is accompanied with an increase in intrinsic activity (Table 1; Fig. 2A). Whereas clobenpropit (**7d**) acts as a partial agonist, the 4-iodo analog **7i** shows full agonism at the H_4R . Furthermore, the dose–response curve of the full agonist **7i** is shifted to the right by the presence of increasing concentrations of **7b** in a competitive manner (slope of the Schild plot = 0.99, $pA_2 = 7.7$, Fig. 2B and C). Remarkably, introduction of an additional chlorine at the 3-position leading to **7g** decreases the H_3R affinity (compare **7d** and **7g**), but highly increases the H_4R affinity (the pK_i H_4R of **7d** and **7g**). The compound has the highest affinity and selectivity for the H_4R among the studied analogs. Moreover, this compound behaves as a full H_4R agonist (α $H_4R = 1$) (Table 1; Fig. 2A).

The structural variation allows us to introduce different properties (i.e., electrostatic, steric, and hydrophobic properties) in the series. The introduction of guanidine (compounds **8a** and **8b**) and isothioureia (compounds **7a–t**) moieties give some differences in the electrostatic properties. The different spacer lengths between the aliphatic amine and the aromatic moiety differentiate the compounds in the steric and hydrophobic properties. The substitution

patterns of the aromatic moieties are also different and these provide some differences in the electrostatic, steric, and hydrophobic properties.

4. Quantitative structure–activity relationships (QSAR)

QSAR equations were generated in order to describe more quantitatively the binding of the ligands to the different receptor subtypes. Eqs. 1 and 2 were generated from the stepwise regression analysis and considered as QSAR models of clobenpropit analogs for ligands of H_4R and H_3R , respectively. Those models have the best statistical significance among the suggested models generated by the stepwise method. A total of 1000 runs of Y-randomization were performed for each QSAR models (Eqs. 1 and 2) to show the distribution of pK_i values. The results show that the internal predictivities (q^2) of the models were better than any of the 1000 scrambled models. Hence, we are confident that the number of examples is enough and heterogenous.

The pK_i H_4R shows a positive correlation with GCUT_SMR_2, E_stb, and dipoleZ, and a negative correlation with SlogP_VSA3 (Eq. 1). The value of the descriptors and the cross correlation between them are presented in Tables 1 and 2 of Supplementary data, respectively. Observed, calculated, and predicted (leave-one-out) affinity values are shown in Supplementary data Table 3 and a correlation between the observed and calculated pK_i is shown in Figure 3A. The leave-one-out method resulted in a cross-validated q^2 of 0.801, which is considered as good.¹¹

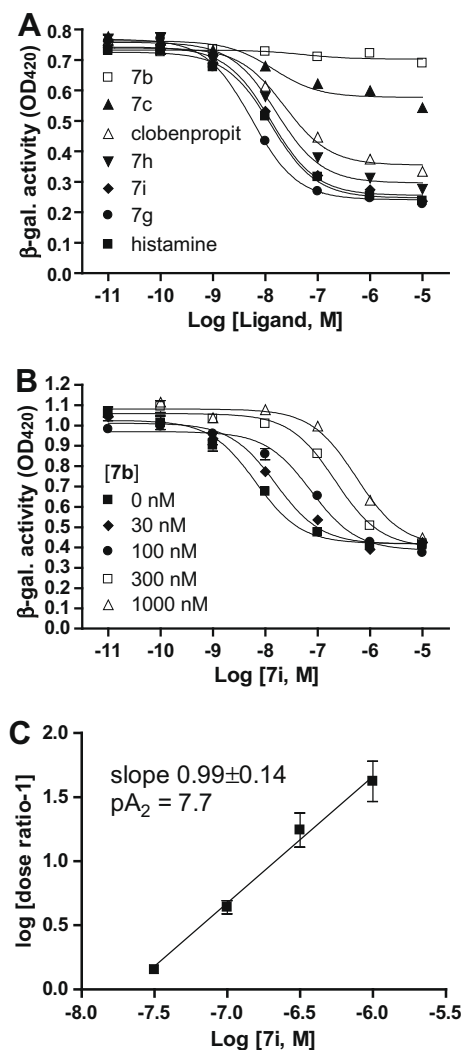


Figure 2. Functional activity of clobenpropit analogs at the human H₄R expressed in SK-N-MC cells, measured as inhibition of forskolin-induced CRE- β -galactosidase activity, (A) Dose-response curves of clobenpropit analogs. (B) Inhibition of **7i** effects by increasing concentrations of **7b**. (C) Schild-plot of antagonism of **7b** against agonist **7i**.

$$\begin{aligned}
 pK_i \text{ H}_4\text{R} = & 5.479 (\pm 0.484) + 9.478 (\pm 1.588) [\text{GCUT_SMR_2}] \\
 & - 0.040 (\pm 0.006) [\text{SlogP_VSA3}] \\
 & + 1.622 (\pm 0.366) [\text{E_stb}] \\
 & + 0.082 (\pm 0.031) [\text{dipoleZ}]
 \end{aligned} \quad (1)$$

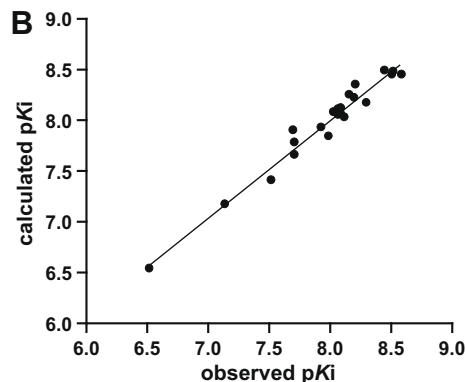
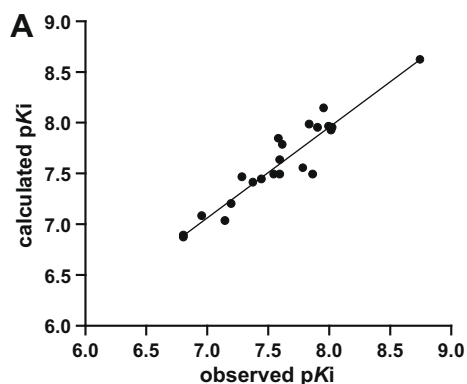


Figure 3. (A) Graph between observed and calculated affinity of clobenpropit analogs for the H₄R. (B) Graph between observed and calculated affinity of clobenpropit analogs for the H₃R.

$N = 22$, $r = 0.946$, $R^2 = 0.894$, $S = 0.166$, $F_{4, 17} = 35.994$, $F_{5\%, 4, 17} = 2.965$, $q^2 = 0.801$.

The definition and the chemical meaning of the relevant descriptors involved in the QSAR models are presented in Table 2. GCUT_SMR_2 is the descriptor calculated from the eigenvalues of a modified graph distance adjacency matrix.^{12,13} The diagonal of the matrix takes the value of the atomic contribution to molar refractivity (using the Wildman and Crippen SMR method).^{13,14} E_stb is the bond stretch-bend cross-term potential energy descriptor calculated from stored 3D conformations, and dipoleZ is the z component of the dipole moment.^{13,15} Since these descriptors show positive correlation, new ligands with high GCUT_SMR_2, E_stb, and dipoleZ value should have better affinity for the H₄R. On the other hand, the negative contribution by SlogP_VSA3 indicates that this property should be minimized in order to obtain more potent H₄R ligands. SlogP_VSA3 is the subdivided surface area descriptor based on the sum of the approximate accessible van der Waal's surface area,¹³ calculated for each atom with contribution to log of partition coefficient (octanol/water) in the range of 0–0.1.¹⁴

Eq. 2 shows that all descriptors, that is, E_sol, BCUT_SLOGP_0, GCUT_PEOE_1, and BCUT_PEOE_2 have a positive contribution in the equation. The correlation between observed and calculated values is presented in the Supplementary data (Tables 4 and 5). Observed, calculated and predicted (leave-one-out) affinity values are shown in Table 6 of the Supplementary data. The correlation between them can be seen in Figure 3B. The leave-one-out method resulted in a cross-validated q^2 of 0.946, which is considered as excellent.¹¹

$$\begin{aligned}
 pK_i \text{ H}_3\text{R} = & 25.349 (\pm 1.897) + 3.816 (\pm 0.375) [\text{E_sol} \times 10^{-3}] \\
 & + 3.702 (\pm 0.360) [\text{BCUT_SLOGP_0}] \\
 & + 23.234 (\pm 4.058) [\text{GCUT_PEOE_1}] \\
 & + 2.998 (\pm 1.016) [\text{BCUT_PEOE_2}]
 \end{aligned} \quad (2)$$

$N = 22$, $r = 0.982$, $R^2 = 0.964$, $S = 0.099$, $F_{4, 17} = 115.091$, $F_{5\%, 4, 17} = 2.965$, $q^2 = 0.946$.

E_sol is the solvation energy descriptor.^{13,15} BCUT_SLOGP_0 and BCUT_PEOE_2 are descriptors calculated from the eigenvalues of a modified distance adjacency matrix.^{13,16} The diagonal of the matrices takes the value of the atomic contribution to log P , and the PEOE partial charge calculated by Gasteiger method, respectively.^{12,14,17} GCUT_PEOE_1 is a descriptor calculated from the eigenvalues of a modified graph adjacency matrix.^{12,13} The diagonal of the matrix takes the value of the PEOE partial charges.^{13,17} The definition and the chemical meaning of these descriptors are presented in Table 2.

Table 2Definition and chemical meaning of the descriptors found for the QSAR models, generated with the QuaSAR descriptor module in MOE 2006.08.¹³

Descriptor	Definition	Chemical meaning
BCUT_PEOE_2	A descriptor calculated from the eigenvalues of a modified distance adjacency matrix. The diagonal of the matrix takes the PEOE ^a partial charges	Steric, electrostatic
BCUT_SLOGP_0	A descriptor calculated from the eigenvalues of a modified distance adjacency matrix. The diagonal of the matrix takes the value of the atomic contribution to log <i>P</i>	Steric, hydrophobic
dipoleZ	The z component of the dipole moment	Electrostatic
E_sol	The solvation energy descriptor	Hydrophobic
E_stb	The bond stretch-bend cross-term potential energy descriptor calculated from stored 3D conformations	Steric
GCUT_PEOE_1	A descriptor calculated from the eigenvalues of a modified graph distance adjacency matrix. The diagonal of the matrix takes the value of the atomic contribution to molar refractivity	Steric, electrostatic
GCUT_SMR_2	A descriptor calculated from the eigenvalues of a modified graph distance adjacency matrix. The diagonal of the matrix takes the value of the atomic contribution to molar refractivity	Steric
SlogP_VSA3	The subdivided surface area descriptor based on the sum of the approximate accessible van der Waal's surface area, calculated for each atom with contribution to log of partition coefficient (octanol/water) in the range of 0–0.1	Hydrophobic

^a PEOE is a partial charge descriptor calculated using the partial equalization of orbital electronegativities.

When the pK_i values for the H₃R were subjected to regression analysis with the parameters which were found for the equation which describe the pK_i for the H₄R (Eq. 2), it was observed that these descriptors show also a statistically significant contribution to the pK_i of the H₃R (Eq. 3). Likewise, when the pK_i values for the H₄R were subjected to regression analysis with the parameters contributing to the pK_i values for the H₃R, it was observed that they also show a statistically significant contribution to the pK_i values for the H₄R (Eq. 4). Both models (Eqs. 3 and 4) explain 75.8% and 56.0% of variances, respectively, underlining that it is difficult to design new clobenpropit analogs as selective ligands of either the H₄R or the H₃R based on these particular descriptors.

$$\begin{aligned}
 pK_i \text{ hH}_3\text{R} = & 5.138 (\pm 0.758) \\
 & + 12.506 (\pm 2.487) [\text{GCUT_SMR_2}] \\
 & - 0.002 (\pm 0.009) [\text{SlogP_VSA3}] \\
 & - 0.625 (\pm 0.573) [\text{E_stb}] \\
 & - 0.073 (\pm 0.048) [\text{dipoleZ}] \quad (3)
 \end{aligned}$$

$$N = 22, r = 0.871, R^2 = 0.758, S = 0.259, F_{4, 17} = 13.327, F_{5\%, 4, 17} = 2.965.$$

$$\begin{aligned}
 pK_i \text{ hH}_4\text{R} = & 17.215 (\pm 6.451) + 0.030 (\pm 1.277) [\text{E_sol} \times 10^{-3}] \\
 & + 4.849 (\pm 1.224) [\text{BCUT_SLOGP_0}] \\
 & - 0.133 (\pm 13.800) [\text{GCUT_PEOE_1}] \\
 & + 4.199 (\pm 3.455) [\text{BCUT_PEOE_2}] \quad (4)
 \end{aligned}$$

$$N = 22, r = 0.748, R^2 = 0.560, S = 0.339, F_{4, 17} = 5.413, F_{5\%, 4, 17} = 2.965.$$

In order to understand the obstacles in designing new clobenpropit analogs as selective ligands of the H₄R, Pearson correlation analysis was performed. This method analyzes the correlation between the descriptors describing the H₃R and the H₄R affinity

Table 3Correlation matrices for descriptors influencing in the H₃R affinity and descriptors influencing in the H₄R affinity

H ₄ R	H ₃ R			
	(+) E_sol	(+) BCUT_SLOGP_0	(+) GCUT_PEOE_1	(+) BCUT_PEOE_2
(+) GCUT_SMR_2	0.725	0.686	0.107	-0.027
(-) SlogP_VSA3	-0.275	-0.852	0.211	0.090
(+) E_stb	-0.438	-0.637	0.061	0.272
(+) dipoleZ	-0.184	-0.159	-0.412	-0.036

respectively (Table 3). Based on Table 3, increasing the H₄R affinity by increasing GCUT_SMR_2 and/or decreasing SlogP_VSA3 will also increase the H₃R affinity by increasing E_sol and BCUT_SLOGP_0. This indicates that GCUT_SMR_2 and SlogP_VSA3 should be considered in designing high affinity ligands for the H₄R, but this modification will not improve the H₄R selectivity toward H₃R. Interestingly, E_stb, has a good negative correlation with BCUT_SLOGP_0. Note that E_stb has a good positive correlation in Eq. 1, and so has BCUT_SLOGP_0 in Eq. 2. This means that increasing the H₄R affinity by increasing E_stb will actually decrease the H₃R affinity. Thus, E_stb, an energy related descriptor, is suggested to be the important property that leads to selectivity for the H₄R within this clobenpropit class of compounds.

5. Conclusions

The synthesis and pharmacological characterization of a series of clobenpropit derivatives are described. The compounds have moderate to high affinity for both the human H₃R and H₄R, and show variable intrinsic activities at the H₄R, ranging from neutral antagonism to full agonism. Both for the H₃R and for the H₄R affinity, QSAR models could be derived. The set of descriptors differs depending on histamine receptor subtype, thereby reflecting their subtle differences in the ligand binding. The QSAR equations reflect that it is not trivial to design clobenpropit derivatives with good selectivity for the H₄R. Nevertheless, the equations indicate that exploring energy related descriptors can be useful to design selective ligands for the H₄R. The series of compounds presented here will serve as useful tools to combine ligand and receptor-based modeling studies.

6. Experimental

6.1. General procedure in synthesis

Chemicals were obtained from commercial suppliers and were used without further purification. ¹H NMR and ¹³C NMR spectra were recorded on a Bruker AC-200 (200 MHz) spectrometer. J. T. Baker silica gel was used for flash chromatography. All melting points are uncorrected and were measured on an Optimelt automated melting point system from Stanford Research Systems. Analytical HPLC-MS analyses were conducted using a Shimadzu LC-8A preparative liquid chromatograph pump system with a Shimadzu SPD-10AV UV-vis detector with the MS detection performed with

a Shimadzu LCMS-2010 liquid chromatograph–mass spectrometer. The buffer mentioned under conditions I and II is a 0.4% (w/v) NH_4CO_3 solution in water, adjusted to pH 8.0 with NH_4OH . The analyses was performed using the following conditions: Condition I: an Xbridge (C18)5 μm column (100 mm \times 4.6 mm) with the following two solvents: solvent A, 90% MeCN–10%; solvent B, 90% water–10% buffer; flow rate = 2.0 ml/min; start: 5% A, linear gradient to 90% A in 10 min, then 10 min at 90% A, then 10 min at 5% A. Total run time: 30 min. Compound purities under both conditions were calculated as the percentage peak area of the analyzed compound by UV detection at 254 nm.

6.2. Synthesis of 3-bromo-2-methoxytetrahydro-2H-pyran (2)

A mixture of 33.65 g (0.4 mol) 3,4-dihydropyran and 36.04 g (0.44 mol) sodium acetate and 100 ml of methanol was cooled to -60°C . Then a bromine (36 ml, 0.4 mol) solution in 100 ml of methanol was added drop wise while the temperature was kept between -50 and -60°C . An additional portion of methanol (100 ml) was added and the reaction mixture was stirred overnight. Water (1000 ml) was added and extracted with a mixture of pentane/diethylether (1/1, v/v) (3×250 ml). The organic layer was washed with of saturated solution of aqueous sodium hydrogen carbonate (500 ml), then with brine (500 ml). The organic layer was dried with magnesium sulfate, filtered, and concentrated in vacuo. This yielded 45 g (58%) of a clear oil that was used without further purification.

6.3. Synthesis of 3-(1H-imidazol-4-yl)propan-1-ol (3)

To a mixture of formamidine acetate (106 g, 0.51 mol) and formamide (550 ml) was added drop wise 3-bromo-2-methoxytetrahydro-2H-pyran (100 g, 0.51 mol) during 90 min. Then the mixture was heated at reflux temperature for 3 h and the formamide removed in vacuo. Raw yield is 125 g. The raw material was purified over an ion exchange column (1.9 mVal ml^{-1} , cap, 1.5 equiv). Final yield: 17 g (26%).

^1H NMR (D_2O) δ 1.76 (m, 2H); 2.00 (t, 2H); 3.60 (t, 2H); 6.71 (s, 1H); 7.57 (s, 1H).

6.4. Synthesis of 4-(3-bromopropyl)-1H-imidazole (4)

To 1H-imidazol-4-yl)propan-1-ol (16.78 g, 0.133 mol) was added 48% hydrobromic acid (100 ml) and heated at reflux temperature for 48 h. Evaporation of the hydrobromic acid gave 16.23 g (90%) of a brown sticky oil that was used without further purification. ^1H NMR (D_2O): δ 2.10–2.25 (m, 2H); 2.88 (t, 2H); 3.47 (t, 2H); 7.23 (s, 1H); 8.55 (s, 1H).

6.5. General procedure of the synthesis of N-benzoyl-N'-R-thiourea (5a-t)

Benzoyl isothiocyanate (1 equiv) was dissolved in diethyl ether and cooled to 0°C . The corresponding R-amine (1.1 equiv) was added drop wise. Then the reaction mixture was stirred at rt for 2 h. The product was collected by filtration, washed with anhydrous diethyl ether, and dried in vacuo. Isolated yields were between 86% and 100%.

6.6. General procedure of the synthesis of N'-R-thiourea (6a-t)

To a solution of the corresponding N-benzoyl-N'-R-thiourea (1 equiv) in ethanol was added potassium carbonate (2 equiv) in water. This mixture was heated at reflux temperature for 3 h. The organic layer was concentrated to half the volume and cooled, after which the product could be collected by filtration of the crystals. The isolated yields were between 47% and 95%.

6.7. General procedure of the synthesis of clobenpropit analogs

Intermediate 4-(3-bromopropyl)-1H-imidazole hydrobromide (1 equiv) was added to the corresponding N'-R-thiourea **6** (1 equiv) in ethanol and heated at reflux temperature for 48 h. After evaporation of the solvent, the salt was purified by column chromatography (ethyl acetate/methanol, 9/1), and crystallized from methanol/ethyl acetate (1/3, v/v) unless indicated otherwise.

6.7.1. 2-[3-(Imidazol-4-yl)-propyl]-1-(benzyl)-isothiourea dihydrobromide (7b)

Isolated yield after recrystallization from ethanol/ethyl acetate, 1:1 is: 25%. Mp: 155–160 $^\circ\text{C}$. ^1H NMR (MeOD): δ 2.03–2.17 (m, 2H); 2.91 (t, $J = 7.5$ Hz, 2H); 3.23–3.38 (m, 2H); 4.61 (s, 2H); 7.22–7.59 (m, 5H); 8.85 (d, $J = 1.3$ Hz, 1H). ^{13}C NMR (200 MHz, MeOD): δ 24.10; 28.88; 31.56; 47.73; 117.29; 128.92 (2C), 129.52; 130.10 (2C); 133.95; 135.03; 135.76; 168.57. HRMS (EI) m/z calcd for $\text{C}_{14}\text{H}_{18}\text{N}_4\text{S}$: 274.1552; found: 274.1248.

6.7.2. 2-[3-(Imidazol-4-yl)-propyl]-1-(4-fluoro-benzyl)-isothiourea dihydrobromide (7c)

Isolated yield after crystallization: 31%. Mp: 197.2–198.2 $^\circ\text{C}$. ^1H NMR (MeOD): δ 2.02–2.17 (M, 2H); 2.92 (t, $J = 7.6$ Hz, 2H); 3.27–3.33 (m, 2H); 4.59 (s, 2H); 7.14 (t, $J = 8.7$ Hz, 2H); 7.37–7.44 (m, 3H); 8.85 (d, $J = 1.3$ Hz, 1H). ^{13}C NMR (MeOD, 8000 scans): δ 24.11; 28.88; 31.59; 47.73; 116.58; 117.02; 117.30; 131.07; 131.24; 131.771; 133.95; 135.01; 166.569 and 168.60 (1C due to Fluor-splitting). HRMS (EI) m/z calcd for $\text{C}_{14}\text{H}_{17}\text{FN}_4\text{S}$: 292.1158; found: 292.1153.

6.7.3. 2-[3-(Imidazol-4-yl)-propyl]-1-(3-chloro-benzyl)-isothiourea dihydrobromide (7e)

Isolated yield after recrystallization from methanol/ethyl acetate (1/1, v/v): 22%. Mp: 200–201 $^\circ\text{C}$. ^1H NMR (MeOD): δ 2.01–2.18 (m, 2H); 2.92 (t, $J = 7.6$ Hz, 2H); 3.27–3.39 (m, 2H); 4.62 (s, 2H); 7.21–7.52 (m, 5H); 8.85 (d, $J = 1.3$ Hz, 1H). ^{13}C NMR (MeOD, 8000 scans): δ 24.12; 28.92; 31.63; 47.75; 117.32; 127.31; 128.89; 129.55; 131.67; 133.94; 135.00; 135.80; 138.13; 168.94. HRMS (EI) m/z calcd for $\text{C}_{14}\text{H}_{17}\text{ClN}_4\text{S}$: 308.0862; found: 308.0852.

6.7.4. 2-[3-(Imidazol-4-yl)-propyl]-1-(2-chloro-benzyl)-isothiourea dihydrobromide (7f)

Isolated yield after recrystallization from methanol/ethyl acetate (1/4 v/v): 25%. Mp: 225–226 $^\circ\text{C}$. ^1H NMR (200 MHz, MeOD): δ 2.04–2.19 (m, 2H); 2.92 (t, $J = 7.6$ Hz, 2H); 3.25–3.36 (m, 2H); 4.68 (s, 2H), 7.36–7.53 (m, 5H); 8.85 (d, $J = 1.3$ Hz, 1H). ^{13}C NMR (MeOD, 8000 scans): δ 24.10; 28.88; 31.66; 47.24; 117.29; 128.75; 131.10; 131.22; 131.50; 133.02; 133.95; 135.04. HRMS (EI) m/z calcd for $\text{C}_{14}\text{H}_{17}\text{ClN}_4\text{S}$: 308.0862; found: 308.0850.

6.7.5. 2-[3-(Imidazol-4-yl)-propyl]-1-(3,4-dichloro-benzyl)-isothiourea dihydrobromide (7g)

Isolated yield after crystallization: 15%. Mp: 217.1–218.0 $^\circ\text{C}$. ^1H NMR (MeOD): δ 2.00–2.18 (m, 2H); 2.92 (t, $J = 7.6$ Hz, 2H); 3.29–3.39 (m, 2H); 4.61 (s, 2H); 7.31 (dd, $J_1 = 6.17$ Hz, $J_2 = 2.07$ Hz, 1H); 7.40 (s, 1H); 7.51–7.62 (m, 2H); 8.84 (d, $J = 1.2$ Hz, 1H). ^{13}C NMR (MeOD, 8000 scans): δ 24.14; 28.87; 31.60; 47.39; 117.29; 128.78; 130.98; 132.17; 133.98; 135.04; 136.58; 169.11. HRMS (EI) m/z calcd for $\text{C}_{14}\text{H}_{16}\text{Cl}_2\text{N}_4\text{S}$: 342.0473; found: 342.0457.

6.7.6. 2-[3-(Imidazol-4-yl)-propyl]-1-(4-bromo-benzyl)-isothiourea dihydrobromide (7h)

Isolated yield after crystallization: 16%. Mp: 202–203 $^\circ\text{C}$. ^1H NMR (MeOD): δ 2.05–2.17 (m, 2H); 2.91 (t, $J = 7.6$ Hz, 2H); 3.20–3.31 (m, 2H); 4.58 (s, 2H); 7.29 (d, $J = 8.5$ Hz, 2H); 7.39 (s, 1H); 7.56 (d, $J = 8.5$ Hz, 2H); 8.84 (d, $J = 1.4$ Hz, 1H). ^{13}C NMR (MeOD,

8000 scans): δ 24.12; 28.86; 31.58; 47.73; 117.29; 123.32; 130.85; 133.18; 133.95; 135.03; 168.83. HRMS (EI) m/z calcd for $C_{14}H_{17}BrN_4S$: 352.0357; found: 352.0337.

6.7.7. 2-[3-(Imidazol-4-yl)-propyl]-1-(4-iodo-benzyl)-isothiourea dihydrobromide (7i)

Isolated yield after crystallization: 26%. Mp: 201.9–202.9 °C. 1H NMR (MeOD): δ 2.02–2.15 (m, 2H); 2.91 (t, $J = 7.60$ Hz, 2H); 3.30–3.40 (m, 2H), 4.57 (s, 2H); 7.15 (d, $J = 8.3$ Hz, 2H); 7.39 (s, 1H); 7.86 (d, $J = 8.3$ Hz, 2H); 8.80 (d, $J = 1.3$ Hz, 1H). ^{13}C NMR (MeOD, 8000 scans): δ 24.19; 28.93; 31.62; 47.60; 94.64; 117.29; 130.92 (2C); 134.09; 135.06; 135.62; 139.27 (2C). HRMS (EI) m/z calcd for $C_{14}H_{17}IN_4S$: 400.0219; found: 400.0208.

6.7.8. 2-[3-(Imidazol-4-yl)-propyl]-1-(4-methyl-benzyl)-isothiourea dihydrobromide (7j)

Isolated yield after crystallization: 15%. Mp: 201.7–203.1 °C. 1H NMR (MeOD): δ 2.02–2.15 (m, 2H); 2.33 (s, 3H); 2.91 (t, $J = 7.5$ Hz, 2H); 3.20–3.38 (m, 2H), 4.55 (s, 2H); 7.00–7.30 (m, 4H); 7.39 (s, 1H); 8.85 (d, $J = 1.4$ Hz, 1H). ^{13}C NMR (MeOD, 8000 scans): δ 21.17; 24.09; 28.89; 31.57; 47.74; 117.29; 128.96 (2C); 130.66 (2C); 132.68; 133.96; 135.02; 139.54; 168.37. HRMS (EI) m/z calcd for $C_{15}H_{20}N_4S$: 288.1409; found: 288.1400.

6.7.9. 2-[3-(Imidazol-4-yl)-propyl]-1-(4-methoxy-benzyl)-isothiourea dihydrobromide (7k)

Isolate yield after crystallization: 29%. Mp: 196.2–196.5 °C. 1H NMR (MeOD): δ 2.04–2.15 (m, 2H); 2.90 (t, $J = 7.6$ Hz, 2H); 3.20–3.33 (m, 2H); 3.79 (s, 3H); 4.51 (s, 2H); 6.94 (d, $J = 8.7$ Hz, 2H); 7.28 (d, $J = 8.6$ Hz, 2H); 7.39 (s, 1H); 8.84 (d, $J = 1.2$ Hz, 1H). ^{13}C NMR (MeOD, 8000 scans): δ 24.86; 29.64; 32.32; 48.50; 56.57; 116.17; 118.03; 128.28; 131.30; 135.80. HRMS (EI) m/z calcd for $C_{15}H_{20}N_4OS$: 304.1358; found: 304.1350.

6.7.10. 2-[3-(Imidazol-4-yl)-propyl]-1-[2-(phenyl)-ethyl]-isothiourea dihydrobromide (7l)

Isolated yield after recrystallization from methanol/ethyl acetate (1/1, v/v): 20%. Mp: 178–183 °C. 1H NMR (200 MHz, MeOD): δ 1.91–2.06 (m, 2H); 2.86 (t, $J = 7.6$ Hz, 2H); 2.97 (t, $J = 7.1$ Hz, 2H); 3.20 (t, $J = 7.3$ Hz, 2H); 3.67 (t, $J = 7.1$ Hz, 2H); 7.09–7.43 (m, 5H); 7.38 (s, 1H); 8.85 (d, $J = 1.4$ Hz, 1H).

^{13}C NMR (200 MHz, MeOD): δ 24.04; 28.80; 31.48; 34.78; 46.45; 117.29; 127.98 (2C); 129.79; 129.95(2C); 133.94; 135.04; 138.91; 168.25. HRMS (EI) m/z calcd for $C_{15}H_{20}N_4S$: 288.1409; found: 288.1409.

6.7.11. 2-[3-(Imidazol-4-yl)-propyl]-1-[2-(4-chloro-phenyl)-ethyl]-isothiourea dihydrobromide (7m)

Isolated yield after crystallization: 27%. Mp: 205 °C. 1H NMR (MeOD): δ 1.91–2.06 (m, 2H); 2.86 (t, $J = 7.7$ Hz, 2H); 2.97 (t, $J = 7.1$ Hz, 2H); 3.22 (t, $J = 7.3$ Hz, 2H); 3.66 (t, $J = 7.1$ Hz, 2H); 7.18–7.32 (m, 4H); 7.39 (s, 1H); 8.85 (d, $J = 1.2$ Hz, 1H). ^{13}C NMR (MeOD, 8000 scans): δ 24.09; 28.85; 31.49; 34.09; 46.18; 117.27; 129.80 (2C); 131.66 (2C); 133.80; 133.95; 135.04; 137.73; 168.37. HRMS (EI) m/z calcd for $C_{15}H_{19}ClN_4S$: 322.1019; found: 322.1003.

6.7.12. 2-[3-(Imidazol-4-yl)-propyl]-1-[2-(4-bromo-phenyl)-ethyl]-isothiourea dihydrobromide (7n)

Isolated yield after crystallization from isopropanol: 25%. Mp: 202–203 °C. 1H NMR (MeOD): δ 1.92–1.99 (m, 2H); 2.74 (t, $J = 7.37$ Hz, 2H); 2.91 (t, $J = 7.0$ Hz, 2H); 3.13 (t, $J = 7.0$ Hz, 2H); 3.63 (t, $J = 7.4$ Hz, 2H); 6.69 (s, 3H); 7.03 (s, 1H); 7.18 (d, $J = 8.4$ Hz, 2H); 7.44 (d, $J = 8.4$ Hz, 2H); 8.07 (s, 1H). ^{13}C NMR (MeOD, 8000 scans): δ 25.38; 29.52; 31.54; 34.22; 46.00; 166.69;

21.74; 131.94; 132.83; 135.69; 136.22; 136.48; 138.24; 171.30. HRMS (EI) m/z calcd for $C_{15}H_{19}BrN_4S$: 366.0514; found: 366.0500.

6.7.13. 2-[3-(Imidazol-4-yl)-propyl]-1-[2-(4-iodo-phenyl)-ethyl]-isothiourea dihydrobromide (7o)

Isolated yield after crystallization: 18%. Mp: 223–225 °C. 1H NMR (200 MHz, MeOD): δ 1.94–2.02 (m, 2H); 2.80–3.01 (m, 4H); 3.21 (t, $J = 7.3$ Hz, 2H); 3.65 (t, $J = 7.1$ Hz, 2H); 7.08 (d, $J = 8.3$, 2H); 7.39 (s, 1H); 7.65 (d, $J = 8.3$ Hz, 2H); 8.86 (d, $J = 1.3$ Hz, 1H). ^{13}C NMR (200 MHz, MeOD, 8000 scans): δ 24.09; 28.83; 31.49; 34.27; 46.06; 92.86; 117.28; 132.19 (2C); 133.92; 135.05; 138.75; 138.94 (2C); 168.37. HRMS (EI) m/z calcd for $C_{15}H_{19}IN_4S$: 414.0375; found: 414.083.

6.7.14. 2-[3-(Imidazol-4-yl)-propyl]-1-[2-(4-methyl-phenyl)-ethyl]-isothiourea dihydrobromide (7p)

Isolated yield after crystallization: 17%. Mp: 219.0–220.6 °C. 1H NMR (MeOD): δ 1.96–2.02 (m, 2H); 2.27 (s, 3H); 2.79–2.98 (m, 4H); 3.20 (t, $J = 7.3$ Hz, 2H); 3.64 (t, $J = 7.1$ Hz, 2H); 7.00–7.21 (m, 4H); 7.37 (s, 1H); 8.82 (s, 1H). ^{13}C NMR (MeOD, 8000 scans): δ 21.10; 24.19; 28.85; 31.50; 34.40; 46.56; 117.26; 129.83 (2C); 130.37 (2C); 134.07; 135.05; 135.76; 137.65; 168.20. HRMS (EI) m/z calcd for $C_{16}H_{22}N_4S$: 302.1565; found: 302.1562.

6.7.15. 2-[3-(Imidazol-4-yl)-propyl]-1-[2-(4-methoxy-phenyl)-ethyl]-isothiourea dihydrobromide (7q)

Isolated yield after crystallization: 30%. Mp: 172–174 °C. 1H NMR (MeOD): δ 1.93–2.00 (m, 2H); 2.72–2.98 (m, 4H); 3.20 (t, $J = 7.3$ Hz, 2H); 3.62 (t, $J = 7.1$ Hz, 2H); 3.74 (s, 3H); 6.85 (d, $J = 8.6$ Hz, 2H); 7.18 (d, $J = 8.6$ Hz, 2H); 7.37 (s, 1H), 8.84 (s, 1H). ^{13}C NMR (MeOD, 8000 scans): δ 24.09; 28.84; 31.49; 33.93; 46.64; 55.71; 115.13 (2C); 117.23; 130.70; 130.95(2C); 135.04. HRMS (EI) m/z calcd for $C_{16}H_{22}N_4OS$: 318.1514; found: 318.1501.

6.7.16. 2-[3-(Imidazol-4-yl)-propyl]-1-(3,3-diphenylpropyl)-isothiourea dihydrobromide (7r)

Isolated yield: 27%. The solid decomposes at 85 °C. 1H NMR (MeOD): δ 1.99–2.13 (m, 2H); 2.39–2.50 (m, 2H), 2.88 (t, $J = 7.5$ Hz, 2H); 3.21 (t, $J = 7.3$ Hz, 2H); 3.23–3.40 (m, 2H), 4.04 (t, $J = 8.0$ Hz, 1H); 7.10–7.47 (m, 11H); 8.71 (s, 1H). ^{13}C NMR (MeOD, 8000 scans): δ 24.33; 28.92; 31.48; 34.23; 44.32; 117.20; 127.67; 128.81 (5C); 129.76 (5C); 134.36; 135.13; 145.11 (2C); 168.31. HRMS (EI) m/z calcd for $C_{22}H_{26}N_4S$: 378.1878; found: 378.1880.

6.7.17. 2-[3-(Imidazol-4-yl)-propyl]-1-[3-(phenyl)-propyl]-isothiourea dihydrobromide (7s)

Isolated yield after recrystallization from ethanol/diethylether (1/1, v/v): 20%. Mp: 177–184 °C. 1H NMR (MeOD): δ 1.88–2.20 (m, 4H); 2.70 (t, $J = 7.7$ Hz, 2H); 2.92 (t, $J = 7.6$ Hz, 2H); 3.14–3.32 (m, 2H); 3.39 (t, $J = 7.2$ Hz, 2H); 7.11–7.33 (m, 5H); 7.41 (s, 1H); 8.84 (d, $J = 1.2$ Hz, 1H). ^{13}C NMR (MeOD): δ 24.12; 28.87; 30.55; 31.49; 33.78; 45.02; 117.29; 127.29; 129.45(2C); 129.61 (2C); 133.96; 135.02; 142.04; 168.23. HRMS (EI) m/z calcd for $C_{16}H_{22}N_4S$: 302.1565; found: 302.1568.

6.7.18. 2-[3-(Imidazol-4-yl)-propyl]-1-[4-phenyl-butyl]-isothiourea dipicrate (7t)

Isolated yield after crystallization from ethyl acetate and petroleum ether (1/1, v/v): 40%. Mp: 112–134 °C. 1H NMR (MeOD): δ 1.60–1.71 (m, 4H); 2.04–2.11 (m, 2H); 2.58–2.72 (m, 2H); 2.89 (t, $J = 7.6$ Hz, 2H); 3.22 (t, $J = 7.3$ Hz, 2H); 3.31–3.41 (m, 2H); 7.09–7.28 (m, 5H); 7.35 (s, 1H); 8.74 (s, 4H); 8.79 (s, 1H). ^{13}C NMR (MeOD, 8000 scans): δ 24.12; 28.38; 28.83; 29.66; 31.39; 36.25; 45.32; 117.15; 126.65(3C); 126.95(2C); 129.38 (4C); 134.00; 135.02. HRMS (EI) m/z calcd for $C_{17}H_{24}N_4S$: 316.1722; found: 316.1721.

6.8. Pharmacology

6.8.1. Radioligand displacement studies

Homogenates of SK-N-MC cells, stably expressing either the human H₃R¹⁸ or the human H₄R,¹⁹ were used for determining ligand affinities for the H₃R and H₄R, respectively, as previously described.²⁰ Cell homogenates of H₃R-expressing cells (475 ± 32 fmol/mg of protein) were incubated for 40 min at 25 °C with 1 nM [³H]-N²-methylhistamine (82 Ci/mmol) in 25 mM Tris HCl buffer containing 145 mM NaCl (pH 7.4), while cell homogenates of H₄R-expressing cells (620 ± 44 fmol/mg of protein) were incubated for 60 min at room temperature with 6–9 nM [³H]histamine (18.1–23.2 Ci/mmol) in 50 mM Tris HCl (pH 7.4), with or without competing ligands. Incubations were terminated by rapid filtration over 96-well GF/C filter plates (Perkin–Elmer Life and Analytical Sciences, Inc., USA) that were pretreated with 0.3% polyethyleneimine. The bound radioligand was subsequently washed using ice-cold wash buffer (H₃R: 25 mM Tris HCl, 145 mM NaCl, pH 7.4 at 4 °C; H₄R: 50 mM Tris HCl, pH 7.4 at 4 °C). The radioactivity retained on the filters was measured by liquid scintillation counting. Nonspecific binding was determined with 1 μM clobenpropit as competing ligand. Competition isotherms were evaluated by a nonlinear, least squares curve-fitting using GraphPad Prism 4.0 (GraphPad Software, Inc., San Diego, CA).

6.8.2. Colorimetric cAMP assay

Colorimetric cAMP assays were performed as previously described.²⁰ Briefly, SK-N-MC cells stably expressing either the human H₃R¹⁸ or human H₄R¹⁹ and a cyclic AMP responsive element (CRE)-β-galactosidase reporter gene were grown overnight in 96-well plates before the assay. To start the assay, the cells were incubated for 6 h with 1 μM forskolin and respective ligands, in triplicates, in a humidified incubator at 37 °C. Thereafter, the medium was aspirated and cells were incubated overnight at room temperature with 100 μl of assay buffer [100 mM NaH₂PO₄, 100 mM Na₂HPO₄, pH 8, 2 mM MgSO₄, 0.1 mM MnCl₂, 0.5% Triton, 40 mM β-mercaptoethanol, and 4 mM o-nitrophenyl-β-D-galactopyranoside (ONPG)]. The absorbance at 420 nm was determined by using a PowerwaveX340 plate reader (Bio-Tek Instruments, Inc., USA).

6.9. Quantitative structure–activity relationship (QSAR) studies

All computational chemistry work was performed using Molecular Operating Environment (MOE) software version 2006.08 developed by Chemical Computing Group, Inc. (Montreal, Canada). A total of 22 compounds were selected for the present study (Table 1). All compounds were built using the builder module of MOE and transferred to the database viewer. Conformational analysis using the stochastic conformation search algorithm was then performed using the conformational import module provided by MOE with no filters and no constraints. The conformational analysis and energy minimization was performed using stochastic conformation search with RMS gradient of 0.001 and iteration limit of 10,000 using a MMFF94 force field.^{13,15,21–23} Descriptors were then calculated.

The relationship between pK_i values at the H₃R or pK_i at the H₄R with the descriptors was identified by stepwise regression analysis using SPSS 14.0 for Windows developed by SPSS, Inc. (Chicago, USA). The following statistical measures were used: *N* = number of samples, *F*-test for quality of fit, *r* = coefficient of correlation, *R*² = coefficient of determination and *S* = standard error of estima-

tion. The descriptors selected for the 'best model' resulting from the stepwise regression analysis should be independent (i.e., the cross correlation between descriptors should not be larger than 0.7; Pearson correlation method was performed to analyze the cross correlation). In case the selected descriptors for the 'best model' were not independent, the relationship was re-examined without the descriptor, which had the lowest correlation with the affinity. The leave-one-out cross-validation (LOO-CV) method was employed to determine cross-validated coefficient (*q*²) as an internal validation of the models. Y-randomization were performed to check the diversity and heterogeneity of the data as well as to investigate the possibility to have a chance correlation in the models.²⁴

Acknowledgments

We thank the Stichting voor de Technische Wetenschappen of the Netherlands Foundation of Scientific Research (Nederlandse Organisatie voor Wetenschappelijk Onderzoek) for financial support through a PIONIER award to Rob Leurs. The histamine H₄R research is supported by COST BM0806 (European Cooperation in Science and Technology). We thank Luc Roumen and Chris de Graaf for technical assistance and helpful discussions.

Supplementary data

Supplementary data associated with this article can be found, in the online version, at doi:10.1016/j.bmc.2009.04.007.

References and notes

- Arrang, J. M.; Garbarg, M.; Schwartz, J. C. *Nature* **1983**, *302*, 832.
- Wijtmans, M.; Leurs, R.; de Esch, I. *Expert Opin. Investig. Drugs* **2007**, *16*, 967.
- Hough, L. B. *Mol. Pharmacol.* **2001**, *59*, 415.
- de Esch, I. J.; Thurmond, R. L.; Jongejan, A.; Leurs, R. *Trends Pharmacol. Sci.* **2005**, *26*, 462.
- Thurmond, R. L.; Gelfand, E. W.; Dunford, P. J. *Nat. Rev. Drug Disc.* **2008**, *7*, 41.
- Sterk, G. J.; van der Goot, H.; Timmerman, H. *Arch. Pharm. (Weinheim)* **1986**, *319*, 624.
- Sterk, G. J.; Koper, J.; Van der Goot, H.; Timmerman, H. *Eur. J. Med. Chem. Chim. Ther.* **1987**, *22*, 491.
- De Esch, I. J.; Mills, J. E.; Perkins, T. D.; Romeo, G.; Hoffmann, M.; Wieland, K.; Leurs, R.; Menge, W. M.; Nederkoorn, P. H.; Dean, P. M.; Timmerman, H. *J. Med. Chem.* **2001**, *44*, 1666.
- de Esch, I. J.; Timmerman, H.; Menge, W. M.; Nederkoorn, P. H. *Arch. Pharm. (Weinheim)* **2000**, *333*, 254.
- Jongejan, A.; Lim, H. D.; Smits, R. A.; de Esch, I. J.; Haaksma, E.; Leurs, R. *J. Chem. Inf. Model.* **2008**, *48*, 1455.
- Eriksson, L.; Jaworska, J.; Worth, A. P.; Cronin, M. T.; McDowell, R. M.; Gramatica, P. *Environ. Health Perspect.* **2003**, *111*, 1361.
- Petitjean, M. *J. Chem. Inf. Comput. Sci.* **1992**, *32*, 331.
- Lin, A. <http://www.chemcomp.com/journal/descr.htm>.
- Wildman, S. A.; Crippen, G. M. *J. Chem. Inf. Comput. Sci.* **1999**, *39*, 868.
- Halgren, T. A. *J. Comput. Chem.* **1996**, *17*, 490.
- Pearlman, R. S.; Smith, K. M. *Perspect. Drug Disc. Des.* **1998**, *9/10/11*, 339.
- Gasteiger, J.; Marsili, M. *Tetrahedron* **1980**, *36*, 3219.
- Lovenberg, T. W.; Roland, B. L.; Wilson, S. J.; Jiang, X.; Pyati, J.; Huvar, A.; Jackson, M. R.; Erlander, M. G. *Mol. Pharmacol.* **1999**, *55*, 1101.
- Liu, C.; Ma, X.; Jiang, X.; Wilson, S. J.; Hofstra, C. L.; Blevitt, J.; Pyati, J.; Li, X.; Chai, W.; Carruthers, N.; Lovenberg, T. W. *Mol. Pharmacol.* **2001**, *59*, 420.
- Lim, H. D.; van Rijn, R. M.; Ling, P.; Bakker, R. A.; Thurmond, R. L.; Leurs, R. *J. Pharmacol. Exp. Ther.* **2005**, *314*, 1310.
- Halgren, T. A. *J. Comput. Chem.* **1996**, *17*, 553.
- Shahapurkar, S.; Pandya, T.; Kawathekar, N.; Chaturvedi, S. C. *Eur. J. Med. Chem.* **2004**, *39*, 899.
- Votano, J. R.; Parham, M.; Hall, L. M.; Hall, L. H.; Kier, L. B.; Oloff, S.; Tropsha, A. *J. Med. Chem.* **2006**, *49*, 7169.
- Rücker, C.; Rücker, G.; Meringa, M. *J. Chem. Inf. Model.* **2007**, *47*, 2345.